Journal of Drug Metabolism and Toxicology

Waring et al., J Drug Metab Toxicol 2012, 3:1
DOI: 10.4172/2157-7609.1000115

Research Article Open Access

Gene Expression Changes Related to Synaptic Deficits in the Tg2576 Mouse Model of Alzheimer's Disease

Jeffrey F. Waring*, David J. Anderson, Paul E. Kroeger, Jinhe Li, Sarah P. Chen, Bradley A. Hooker, Murali Gopalakrishnan and Clark A. Briggs

Neuroscience Research, Abbott Laboratories, Abbott Park, IL, USA

Abstract

Aβ in the form of soluble oligomers or amyloid deposits has been identified as an endogenous substance responsible for the induction of neurodegeneration in Alzheimer's disease. To study Aβ-related processes, we evaluated both input-output electrophysiology and gene expression in hippocampi from Tg2576 and wild-type control mice 7 months of age. In hippocampal CA1 f-EPSP recordings, the postsynaptic response was reduced in Tg2576, while there was no significant difference in fiber volley amplitude or paired-pulse facilitation. Gene expression was evaluated on RNA extracted from hippocampi contralateral to those used for electrophysiology. Robust gene expression differences were observed between Tg2576 and WT hippocampi, many of which reflected deficits in glutamatergic synaptic transmission. These results support the identification of synaptic deficits in young adult Tg2576 mice, and identify gene products that potentially could be used as biomarkers for Aβ toxicity or as mechanistic targets in further studies.

Keywords: Alzheimer's disease; Tg2576; Gene expression; Microarray; Electrophysiology; Hippocampus

Abbreviations: AD: Alzheimer's disease; APP: amyloid precursor protein; f-EPSP: field excitatory postsynaptic potential; FV: fiber volley; LTP: long-term potentiation; OD: optical density; WT: wild-type

Introduction

Deficits in cognitive function remain a major focus in CNS research and drug discovery with prominent foci in Alzheimer's disease (AD), other forms of senile dementia, and cognitive dysfunction associated with disorders such as schizophrenia and Parkinson's disease. AD itself demonstrates a huge impact worldwide and a clear need for treatments more effective than currently available agents. The mechanism(s) underlying the pathogenesis of AD are not known. However, clearly it is a neurodegenerative disorder, and many identify Aβ in the form of soluble oligomers or amyloid deposits as the endogenous substance(s) responsible for its induction. Indeed, familial forms of AD have been linked to specific mutations in the amyloid precursor protein (APP) or in the enzymes responsible for processing APP. The known familial forms of AD account for only a fraction of all known cases, with sporadic AD being much more prevalent. However, it is possible that Aβ aggregates may be induced through mechanisms other than precursor or enzymatic mutation, or that similar pathogenic processes may be induced by substances more varied than a specific Aβ form. Thus, the study of Aβ pathogenic mechanisms may provide further insight into the cause and cure of AD, and research has been driven to understand how Aβ is produced, how aggregates form, how to increase the clearance of toxic species, and how to reverse the neurodegenerative processes induced by AB [1,2].

To study Aβ pathology, a number of transgenic mouse models have been generated. Among these, the Tg2576 mouse was generated by Hsiao to express the Swedish mutation of human APP [3,4]. These animals were found to develop behavioral deficits and insoluble amyloid as young as 6 months, although definitive plaque formation generally is seen only in older animals. Additionally, a deficit in hippocampal dendritic spine synapses, consistent with a neurodegenerative effect, has been observed in the younger Tg2576 [5]. However, deficits in hippocampal synaptic transmission were relatively subtle in earlier electrophysiological studies. In *in vitro* hippocampal slices from aged (> 15 month) Tg2576, Chapman observed deficits in long-term potentiation (LTP) plasticity but not in synaptic strength as reflected by field excitatory postsynaptic potential (f-EPSP) input-output relationship [6]. Fitzjohn, however, did not observe an LTP deficit but did observe a small deficit the in f-EPSP input-output relationship in hippocampal slices from aged Tg2576 [7]. Recently, however, Jacobsen observed deficits in both LTP and the f-EPSP input-output relationship [5]. Additionally, deficits in dendritic spine synapse density and in behavioral performance were observed in Tg2576 as young as 4 months. These data are suggestive of neurodegenerative synaptic loss that may be induced by soluble forms of Aβ, contributing to ensuing cognitive deficits. However, the mechanisms responsible for neurodegeneration and synaptic loss in Tg2576 are not yet clear. In order to identify such pathways, the present study used a combination of electrophysiological and microarray approaches to determine functional and gene expression changes in Tg2576. Hippocampal synaptic strength was assessed electro physiologically *in vitro* in each of the same mice that were used for gene expression analysis. Consistent with Jacobsen, a clear deficit in f-EPSP synaptic strength was observed in 7-month old Tg2576 mice [5]. Further, the study identified a number of gene expression alterations consistent with these synaptic deficits.

***Corresponding author:** Jeffrey F. Waring, Abbott Laboratories, 100 Abbott Park Rd., Abbott Park, IL 60064, Telephone 847-935-4124; Fax 847-935-7845; E-mail: jeff.waring@abbott.com

Received November 07, 2011; **Accepted** January 03, 2012; **Published** January 04, 2012

Citation: Waring JF, Anderson DJ, Kroeger PE, Li J, Chen SP, et al. (2012) Gene Expression Changes Related to Synaptic Deficits in the Tg2576 Mouse Model of Alzheimer's Disease. J Drug Metab Toxicol 3:115. doi:10.4172/2157-7609.1000115

Materials and Methods

Animals

Male Tg2576 and wild-type (WT) littermate control mice were obtained from Taconic Farms (001349-T and 001349-W), housed individually, and treated according to AALAC standards using protocols approved by Abbott's Institutional Animal Care and Use Committee.

Tissue preparation

Mice (27-30 weeks old) were euthanized individually by decapitation under sevoflurane anesthesia. For preparation of brain slices, a high-Mg ACSF (composition, 130 mM NaCl, 1.25 mM NaH_2PO_4, 2.8 mM KCl, 26 mM $NaHCO_3$, 1.0 mM $CaCl_2$, 10 mM $MgCl_2$ and 10 mM dextrose (pH 7.4) was used. The brain was rapidly removed, placed in ice-cold high-Mg ACSF and allowed to chill for 5 minutes before further dissection. The cerebellum was removed and the brain was bisected sagitally. The right half brain was divided into hippocampus, prefrontal cortex and midbrain; each portion was immediately frozen in prechilled tubes on dry ice and later transferred to –80˚C storage for microarray studies. The left half brain sectioned coronally for mounting on a vibratome stage, and 350 µm coronal hippocampal slices were cut and trimmed in high-Mg ACSF at 1˚C. Slices were transferred to normal ACSF at 32˚C and preincubated for ≥ 60 minutes prior to conducting electrophysiological measurements. Each day, one Tg2576 and one WT mice were used, one in the morning and one in the afternoon with the sequence reversed on succeeding days.

Electrophysiological measurements and analysis

Electrophysiological recordings were conducted in artificial cerebrospinal fluid (ACSF) equilibrated with 95% O_2 5% CO_2 and containing 130 mM NaCl, 1.25 mM NaH_2PO_4, 2.8 mM KCl, 26 mM $NaHCO_3$, 2.5 mM $CaCl_2$, 1.3 mM $MgCl_2$ and 10 mM dextrose (pH 7.4). Extracellular f-EPSP recordings were obtained in hippocampal CA1 stratum radiatum in normal ACSF at 32˚C using a Fine Science Tools tissue chamber with the top of the slice at the ACSF/humidified atmosphere interface. Stimulating electrode (stainless steel bipolar, FHC model CE2D75) and recording electrode (glass capillary filled with 2 M NaCl, 1-2 megohm resistance) were placed ~ 300 µm apart (measured with a reticule in a stereo zoom dissecting microscope) along a path roughly parallel to the pyramidal cell layer. The proximity between stimulating and recording electrodes was determined from preliminary experiments to ensure the ability to reliably obtain measurable responses at low stimulus intensity (for input-output curves) from most Tg2576 slices. Some degree of electrode placement optimization was necessary in order to obtain satisfactory responses. Nevertheless, between slices and between animals, care was taken to position electrodes at the same distance and in a similar region of hippocampus CA1 stratum radiatum in order not to skew comparison between Tg2576 and WT animals. Recordings were obtained from 2-4 hippocampal slices from each animal (26 Tg2576 and 23 WT slices) in order to reduce the effect of inter-slice variability on the animal-to-animal comparison.

Stimuli were 200 µs duration constant current pulses of variable intensity in the range of 5-100 A (WPI model DS8000 stimulator and DLS100 stimulus isolation unit). Responses were recorded with 1000x gain, 2 KHz lowpass filter (Axon Instr. Geneclamp 500B with HS2A x10MG headstage), digitized (Axon Instr. Digidata 1322A) and stored and analyzed using Clampex and Clampfit software (Axon Instr. pClamp 9). Statistical analyses and graphs were constructed using Graphpad Prism version 4.03 (Graphpad Software).

In each slice, experiments were conducted in the following sequence: (a) f-EPSP responses were optimized and monitored for stability using 200 µs 50 µA single stimuli; (b) the f-EPSP stimulus-response input-output relationship was determined using 5, 10, 15, 20, 30, 40 50, 70 and 100 µA stimuli; (c) responses to 50 µA stimuli were measured again to determine stability relative to responses obtained before the input-output determination; (d) stimulus intensity was adjusted to obtain f-EPSP responses 50% of maximal amplitude; (e) using the 50% stimulation, paired-pulse facilitation (PPF) was determined using an automated protocol that delivered stimuli at progressively reduced intervals of 200, 150, 100, 50, 20 and 10 ms. Each recording was an average of 3 individual responses, or pair of responses, obtained in succession at 15-s intervals.

Aβ measurement

Plasma from the wildtype and Tg2576 mice used in this study was applied in the Aβ1-40 and Aβ1-42 ELISA. Aβ1-40 ELISA was performed in a 1:5 dilution using 6E10 (Signet, Catalog No 9320, Dedham, MA) as the capture antibody, Rabbit anti-Aβ1-40 (Signet, Catalog No 9130, Dedham, MA) as the detection antibody, and goat-anti rabbit antibody conjugated with horse radish peroxidase (Jackson ImmunoResearch, Catalog No 111-035-144) as the secondary antibody. The 96-well microplate (Corning, Catalog No 3590, Corning, NY) was coated with the capture antibody (200ng/50ml/well) in 0.1 M $NaHCO_3$ pH 8.2 overnight at 4°C. The coated plate was washed 3 times with 200ml/well PBS-T (0.05% Tween 20 in PBS), and blocked with 100ml/well blocking buffer (PBS-T with 1% BSA) for 1 h at room temperature. The plate was then incubated with 25 ml/well standard or samples, and 25 ml/well detection antibody mix (400 ng/ml detection antibody and 1:1000 secondary antibody in blocking buffer) for 1 h at room temperature. The plate was washed 6 times with 250 ml/well PBS-T and incubated with 50ul/well TMB (KEM EN TEC Diagnostic, Catalog No 4380H, Denmark) for 10 min at room temperature followed by 50 µl/well 1 N H_2SO_4. The plate was read for optical density (OD) at 450nm. The OD values were back calculated to concentrations with the standard curve using GraphPad Prism (GraphPad Software). The Aβ1-42 ELISA was performed in a 1:10 dilution using the BetaMark x-42 ELISA Kit (Covance, #SIG-38952; LOT 08GK01325) according to the manufacturer's instructions.

RNA Microarray measurements and analysis

The hippocampus was isolated from the mouse brain and immediately flash-frozen in liquid nitrogen for subsequent RNA isolation. RNA was isolated from the hippocampus using standard TRIzol protocol (Invitrogen Life Technologies). RNA integrity was evaluated using an Agilent bioanalyzer (Agilent Technologies, Model 2100, Foster City, CA). Microarray analysis was performed using the standard protocol provided by Affymetrix, Inc. (Santa Clara, CA), and as performed previously [8]. Briefly, approximately 15 mg of total RNA was reverse transcribed into cDNA using a Superscript II Double-Strand cDNA synthesis kit (Invitrogen Life Technologies) according to the manufacturer's instructions with the exception that the primer used for the reverse transcription reaction was a modified T7 primer

with 24 thymidines at the 5' end (Affymetrix). The sequence was 5'GGCCAGTGAATTGTAATACGAC-TCACTATAGGGAGGCGG-(dT)24-3'. cDNA was purified via phenol/chloroform/isoamylalcohol (Invitrogen Life Technologies) extraction and ethanol precipitation. The purified cDNA was resuspended in molecular biology grade water. Following this procedure, biotin labeled cRNA was synthesized from the cDNA according to the manufacturer's instructions using the Enzo RNA Transcript Labeling Kit (ENZO Life Sciences, Farmindale, NY). The labeled cRNA was then purified using RNeasy kits (Qiagen, Valencia, CA). Subsequently, cRNA concentration and integrity were evaluated. Approximately 20 mg of cRNA was then fragmented in a solution of 40 mM Tris-acetate, pH 8.1, 100 mM KOAc, and 30 mM MgOAc at 94°C for 35 minutes. Fragmented, labeled cRNA was hybridized to an Affymetrix mouse 430A_2 array, which contains sequences corresponding to roughly 22,690 transcripts, at 45°C overnight using an Affymetrix Hybridization Oven 640. The array was subsequently washed and stained twice with strepavidin-phycoerythrin (Molecular Probes, Carlsbad, CA) using the Gene-Chip Fluidics Workstation 400 (Affymetrix). The array was then scanned using the Affymetrix GeneChip® Scanner 3000. The microarray scanned image and intensity files (*.cel files) were imported in Rosetta Resolver gene expression analysis software version 5.0 (Rosetta Inpharmatics, Seattle, WA).

Gene expression analysis was conducted using the Rosetta Resolver software version 5.0. Genes were considered as significantly regulated if they had a p-value of 0.05 or less, in at least 5 out of 7 animals in the treatment group.

Results

Aβ levels

Plasma levels of human Aβ1-40 and Aβ1-42 were assayed by ELISA. All Tg2576 mice used in the study displayed detectable levels of both Aβ species. No detectable levels of human Aβ1-40 or Aβ1-42 were found in wildtype (WT) controls (data not shown).

Electrophysiology

Extracellular recordings in hippocampal CA1 stratum radiatum were obtained from 26 slices of WT mice (n =7 animals) and 23 slices of Tg2576 mice (n = 7 animals) of equivalent ages. As shown in (Figure 1), the field excitatory postsynaptic potential (f-EPSP) response to stimulation of Schaffer collaterals in Tg2576 mice was about half as large as the f-EPSP responses from WT mice. However, the sensitivity to electrical stimulation was not reduced, with the current required for half-maximal f-EPSP amplitude being 17 μA ± 3 μA (mean ± SEM) in Tg2576 compared to 19 ± 2 μA in WT slices.

The fiber volley (FV) amplitude, representing activation of the Schaffer collaterals, could be detected in most Tg2576 WT slice recordings. In 13 Tg2576 slices and 18 WT slices, the FV was well-resolved from both the falling phase of the stimulus artifact and the rising phase of the f-EPSP and could be accurately measured up to 50 μA stimulus current. Unlike the f-EPSP (Figure 1), the FV input-output relationship (Figure 2) did not differ significantly between Tg2576 and WT. These results suggest a deficit in synaptic transmission in Tg2576, but not in excitability of the Schaffer collaterals or in the number of Schaffer collaterals activated by a given stimulus. Consistent with this would be a synaptic deficit due to reduced transmitter release, reduced postsynaptic excitability, or fewer terminals per axon in Tg2576.

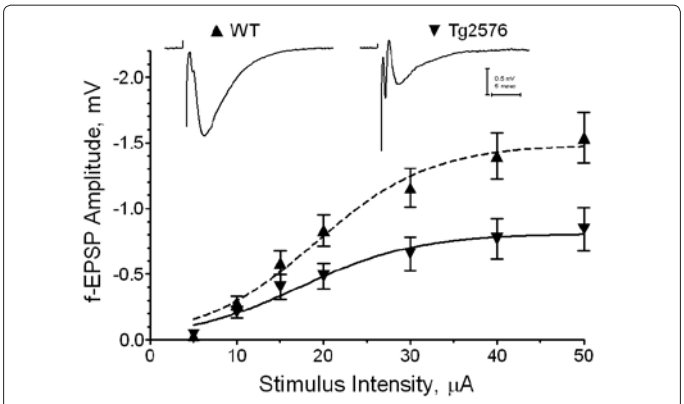

Figure 1: Input-output curves showing reduced hippocampal transmission in Tg2576 mice. The graph shows f-EPSP amplitudes (mean ± SEM) as a function of stimulus intensity in the CA1 stratum radiatum. Sensitivity to electrical stimulation was similar between Tg2576 and WT mice, while response amplitudes, including the maximal response at 50 μA, were, on average, lower in Tg2576. Curves fit to the data were significantly different by global analysis F-test (P < 0.0001). The insets show example responses from WT (left) and Tg2576 (right) slices. Scale bars represent 0.5 mV by 5 ms and apply to both traces.

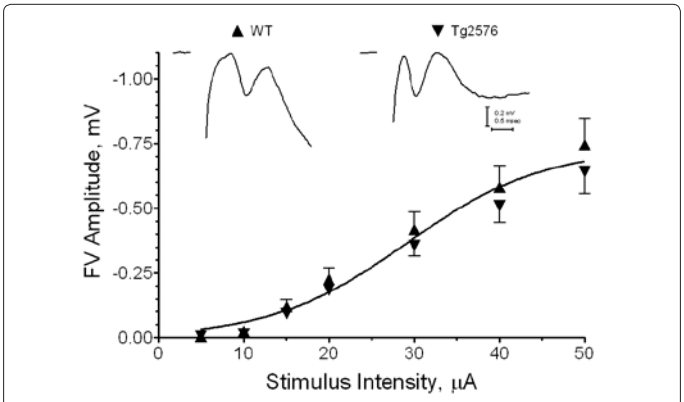

Figure 2: Input-output curves showing unaffected Schaffer collateral afferent responses in Tg2576 mice. The graph shows presynaptic fiber volley (FV) response amplitudes (mean ± SEM) as a function of stimulus intensity in the CA1 stratum radiatum. Curves fit to the data were not significantly different and, while plotted separately, are indistinguishable in the graph shown. The insets show example FV responses from WT (left) and Tg2576 (right) slices. Scale bars represent 0.2 mV by 0.5 ms and apply to both traces.

In the same slices, we also evaluated paired-pulse facilitation at various intervals with the stimulus intensity tuned to elicit a half-maximal initial f-EPSP response in each slice. As demonstrated in (Figure 3), although the Tg2576 f-EPSPs were smaller, nevertheless the degree of paired-pulse facilitation was similar between Tg2576 and WT at intervals between 10 and 200 ms. Thus, short-term plasticity as reflected by paired-pulse facilitation did not appear to be affected in Tg2576.

Gene expression analysis

In light of the decreased synaptic transmission observed in Tg2576 mice relative to WT controls, microarray gene expression analysis was conducted using hippocampi from the Tg2576 and WT mice. For each probe in the array, the expression level in each Tg2576 mouse hippocampus was compared to the mean WT expression level. To distill the changes detected, we applied the criteria that the apparent

change in expression had to be statistically significant ($P < 0.05$) in at least 5 of the 7 mice, and that the change had to be in the same direction in all mice. Accordingly, robust, consistent differences were observed for 452 gene probes across at least 70% (5/7) of the Tg2576 mice (Figure 4). Several genes potentially mechanistically related to synaptic deficits were identified.

The gene expression changes were analyzed using the Ingenuity Pathway Analysis System. Using this system, one can determine which biological pathways are most significantly impacted by the regulated genes. (Figure 5) shows that, from the 452 genes consistently differentially regulated between the Tg2576 and WT mice, the 3 pathways most significantly impacted are synaptic long-term potentiation, calcium signaling and glutamate receptor signaling.

Several genes that are required for glutamate transmission, both presynaptically and postsynaptically including AMPA1, 2 and 3, and the NMDA receptor 1 were down regulated in the majority of Tg2576

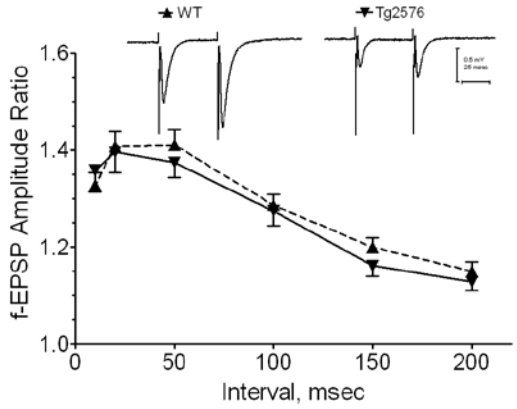

Figure 3: Graph showing unaffected paired-pulse facilitation in Tg2576. In each hippocampal slice, facilitation was tested using pairs of stimuli at intervals ranging from 200 ms to 10 ms. While responses were smaller in Tg2576, the degree of facilitation, measured by the ratio of the response to the second stimulus compared to the first stimulus in each pair, was similar in Tg2576 compared to WT slices. The inset shows examples responses recorded using 50 ms interval paired pulses from a WT slice (left) and a Tg2576 slice (right). Scale bars represent 0.5 mV by 25 ms for both traces.

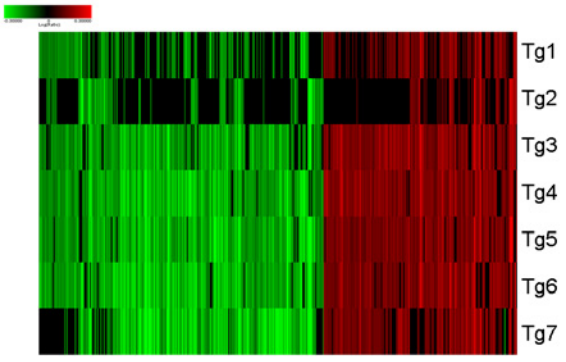

Figure 4: Heatmap showing gene expression changes in hippocampus from Tg2576 mice relative to WT controls. The heatmap shows individual expression profiles from Tg2576 mice relative to an in silico pool of WT control mice. The genes shown (452) were significantly regulated, with a p-value of 0.05 or less in at least 5 Tg2576 mice. Genes shown in green are downregulated, while genes shown in red are upregulated relative to WT controls. Genes shown in black were not significantly changed in expression.

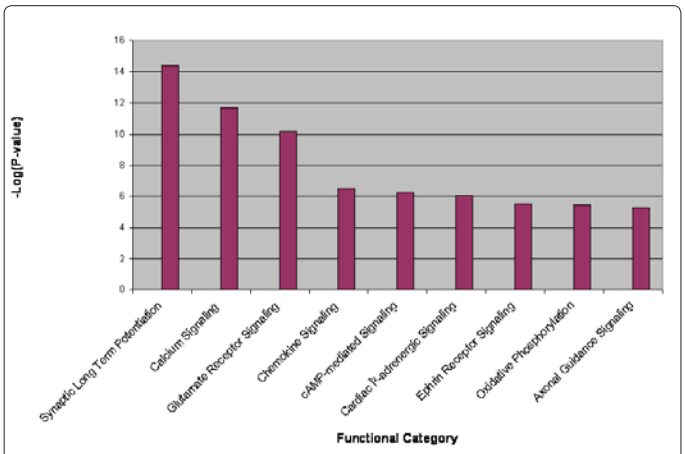

Figure 5: Significantly impacted biological pathways in 7 month old Tg2576 Mice. The 452 genes that were significantly differentially expressed between Tg2576 mice and WT controls were analyzed using the Ingenuity software. The most significantly impacted pathways are shown in the graph. The Y-axis shows the –Log p-value.

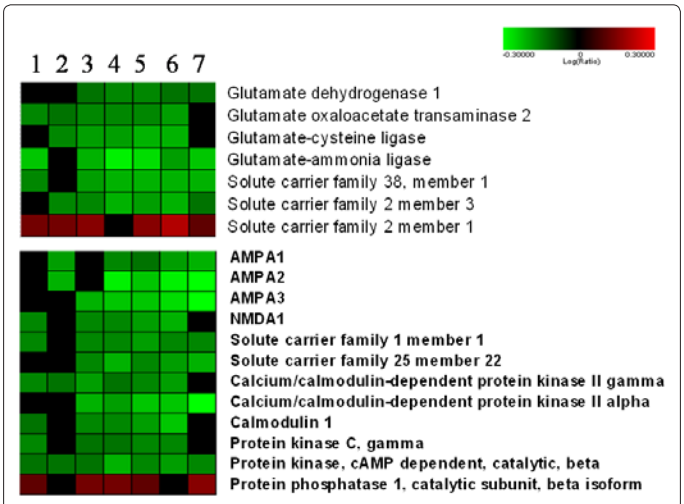

Figure 6: Heatmap showing differentially expressed genes in hippocampus from Tg2576 mice relative to WT controls that are involved in glutamate transmission, both presynaptically and postsynaptically. The heatmap conditions are the same as in Figure 4.

mice relative to WT controls (Figure 6). In addition, the genes encoding the excitatory amino acid transporters solute carrier family 1 member 1 (EAAC1) and solute carrier family 25 member 22 (mitochondria) were down regulated in Tg2576 mice [9-11]. Previous studies have shown that the expression of EAAC1 is regulated by protein kinase C, which was also down regulated in Tg2576 mice. In addition, the GLUT3 gene (solute carrier 2, member 3), which is one of the principle proteins responsible for the transport of glucose into neurons, also was down regulated in Tg2576 hippocampus relative to WT controls [12].

Two isoforms of CaMKII, alpha and gamma, were regulated in Tg2576 mice, relative to WT controls. Other genes that have been shown to be downstream of the AMPA and NMDA receptors and to be involved in post-synaptic transmission, such as protein kinase cAMP dependent beta, calmodulin and protein phosphates 1 were all regulated in Tg2576 relative to WT mice.

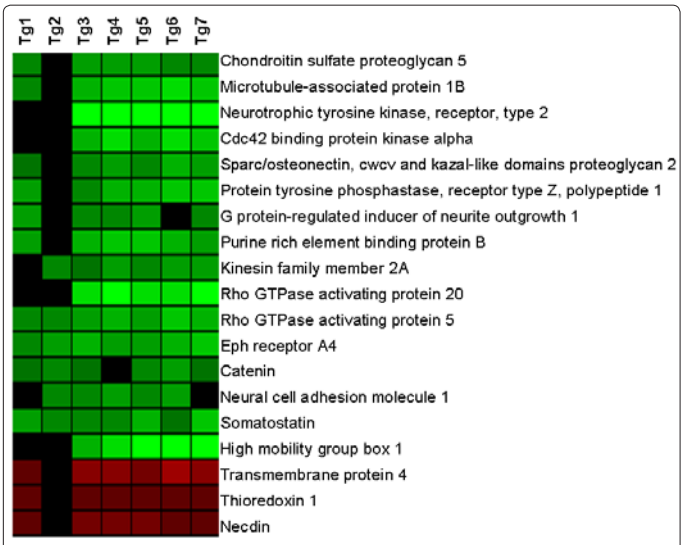

Figure 7: Regulation of genes involved with neurite outgrowth. The heatmap shows differentially expressed genes in hippocampus from Tg2576 mice relative to WT controls that have been shown in the literature to have a role in dendritic spine regulation and neurite outgrowth.

One of the pathways regulated by the 452 genes is the axonal guidance pathway. Previous studies have demonstrated that Tg2576 mice display deficits in dendritic spine density and structure [5,13,14]. In light of this, it was of interest to determine if genes that are associated with dendritic spine regulation and neurite outgrowth were altered in Tg2576 mice. (Figure 7) shows that a number of genes that have been shown to function in dendritic spine function or structure were downregulated in Tg2576 mice relative to WT controls. These include genes encoding for Eph receptor A4 [15], catenin, Cdc42 binding protein kinase [16], purine rich element binding protein B [17], CaMKII [18] and the Rho GTPase [19,20].

Discussion

The results from our study are consistent with the findings from Jacobsen confirming that 7-month old Tg2576 mice show a significant decrease in f-EPSP responses relative to WT controls [5]. Amyloid plaque deposition in Tg2576 mice is generally not observed until 9-12 months of age [21]. These results indicate that the decrease in f-EPSP responses in 7-month old Tg2576 are not a result of plaque formation, and suggest preplaque Aβ oligomers are able to initiate neuronal dysfunction in this animal model. Similar results showing synaptic transmission deficits have been observed in other mouse models with over-expression of amyloid beta [22].

In order to better understand potential molecular mechanisms underlying the decrease in f-EPSP responses in Tg2576 mice, we conducted microarray analysis in hippocampus from the mice used in our study. We observed a significant number of gene expression changes in Tg2576 mice relative to WT controls. In one mouse (Tg2, there appeared to be fewer gene expression changes relative to the other mice, however, this was not reflected in the synaptic deficit recordings or in the levels of plasma Aβ (data not shown).

Many of the gene expression changes were highly consistent between the seven Tg2576 mice used in the study. This finding is of interest since, unlike some other tissues, the brain is composed of highly diverse cell types, thus making identification of distinct gene expression changes challenging. Furthermore, genes that encode proteins responsible for neuronal function, such as neurotransmitter receptors, are expressed at very low levels and the gene expression changes generally have a low magnitude [23,24]. The fact that Tg2576 mice display a large number of very consistent gene expression changes relative to WT controls is consistent with the electrophysiology results, suggesting that the Tg2576 mice have cognitive changes before the onset of amyloid plaques.

Some of the observed gene expression changes may be involved in the mechanism of the EPSP decline observed in Tg2576 mice. Glutamate is the principal excitatory neurotransmitter in the central nervous system. In the hippocampus, glutamate drives the f-EPSP by activation of AMPA-sensitive receptors expressed postsynaptically in dendritic spine synapses and can activate NMDA-sensitive receptors leading to AMPA-sensitive receptor insertion and long-term potentiation (LTP) of synaptic transmission [25,26]. The microarray results showed that genes encoding AMPA receptors 1, 2 and 3, as well as the gene encoding the NMDA receptor 1 were all down regulated in Tg2576 mice relative to WT controls. These results are similar to recent studies conducted using a double transgenic mice, where the authors observed a decrease in AMPA receptor efficacy, at an early age, as measured by evoked AMPA receptor EPSCs, spontaneous AMPA receptor mEPSCs, and evoked f-EPSPs [27]. A decrease in transcription of the AMPA receptors, possibly mediated by soluble Aβ, would result in a decrease in LTP and memory function, which may initiate the early stages of AD. The results suggest that certain AMPA receptors may be a viable target for drug therapy for AD and other dementias.

Studies have shown that calcium/calmodulin dependent protein kinase II (CaMKII), together with other protein kinases, phosphorylates and regulates the functioning of postsynaptic AMPA receptors [28,29]. In addition, it has previously been shown that transcriptional regulation of CaMKII can be regulated by NMDA receptor activity [30]. The microarray results showed that two isoforms of CaMKII, alpha and gamma, were downregulated in Tg2576 mice, relative to WT controls. Previous studies have shown a decrease in the expression of this protein in the frontal cortex and hippocampus of Alzheimer's disease brains [31]. In another study, it was shown that CaMKII-α-expressing neurons were selectively lost in the CA1 subfield of AD patients. Furthermore, CaMKII-α knock-out mouse show deficits in long-term potentiation in hippocampus as well as disrupted spatial learning ability [32,33]. Thus, the down regulation of CaMKII in Tg2576 mice may be a mechanism for the decreased EPSP responses in Tg2576 mice.

In our studies, we combined gene expression analysis with electrophysiology recordings from the same animal. In this way, we were able to focus on gene expression changes related to the synaptic deficits observed, such as changes in glutamate receptors and CaMKII. We also observed gene expression changes in Tg2576 mice that have been seen in previous gene expression analysis. In one study, Reddy examined gene expression changes in Tg2576 mice relative to wildtype controls, at ages ranging from 2 months up to 18 months [34]. Among other changes, the study revealed significant gene expression changes in genes involved in mitochondrial function. In our study, we also observed upregulation of genes such as cytochrome c oxidase, programmed cell death, and ATPase V1 subunit D. As suggested by Reddy, the upregulation of these genes may be a compensatory response to mitochondrial impairment [34,35]. In another study, Wu

studied the gene expression changes in 3 different mouse models of Alzheimer's, including Tg2576 mice [24]. Among other changes, they observed an upregulation in genes involved in proteolysis, such as cathepsin H, D and S. In our study, we also identified an upregulation in cathepsin S in the Tg2576 mice, although changes in other cathepsins were not significant.

The total (452) gene expression changes observed in Tg2576 mice, or a subset of them, may ultimately prove useful as biomarkers for new drug therapy for AD. Currently, it is difficult to measure efficacy of new drug candidates at early ages in Tg2576 mice. By screening for compounds that normalize the expression of altered genes or proteins, it may be possible to identify new drug candidates that would show efficacy in halting or reversing the effects of Alzheimer's disease at an early stage.

Acknowledgements

This work was supported by Abbott Laboratories.

References

1. Klein WL (2002) ADDLs & protofibrils--the missing links? Neurobiol Aging 23: 231-235.
2. Tanzi RE (2005) The synaptic Abeta hypothesis of Alzheimer disease. Nat Neurosci 8: 977-9.
3. Hsiao K, Chapman P, Nilsen S, Eckman C, Harigaya Y, et al. (1996) Correlative memory deficits, Abeta elevation, and amyloid plaques in transgenic mice. Science 274: 99-102.
4. Westerman MA, Cooper-Blacketer D, Mariash A, Kotilinek L, Kawarabayashi T, et al. (2002) The relationship between Abeta and memory in the Tg2576 mouse model of Alzheimer's disease. J Neurosci 22: 1858-67.
5. Jacobsen JS, Wu CC, Redwine JM, Comery TA, Arias R, et al. (2006) Early-onset behavioral and synaptic deficits in a mouse model of Alzheimer's disease. Proc Natl Acad Sci U S A 103: 5161-6.
6. Chapman PF, White GL, Jones MW, Cooper-Blacketer D, Marshall VJ, et al. (1999) Impaired synaptic plasticity and learning in aged amyloid precursor protein transgenic mice. Nat Neurosci 2: 271-6.
7. Fitzjohn SM, Morton RA, Kuenzi F, Rosahl TW, Shearman M, et al. (2001) Age-related impairment of synaptic transmission but normal long-term potentiation in transgenic mice that overexpress the human APP695SWE mutant form of amyloid precursor protein. J Neurosci 21: 4691-8.
8. Liguori MJ, Anderson MG, Bukofzer S, McKim J, Pregenzer JF, et al. (2005) Microarray analysis in human hepatocytes suggests a mechanism for hepatotoxicity induced by trovafloxacin. Hepatology 41: 177-86.
9. Davis KE, Straff DJ, Weinstein EA, Bannerman PG, Correale DM, et al. (1998) Multiple signaling pathways regulate cell surface expression and activity of the excitatory amino acid carrier 1 subtype of Glu transporter in C6 glioma. J Neurosci 18: 2475-85.
10. Mackenzie B, Erickson JD (2004) Sodium-coupled neutral amino acid (System N/A) transporters of the SLC38 gene family. Pflugers Arch 447: 784-95.
11. Trotti D, Peng JB, Dunlop J, Hediger MA (2001) Inhibition of the glutamate transporter EAAC1 expressed in Xenopus oocytes by phorbol esters. Brain Res 914: 196-203.
12. Nagamatsu S, Kornhauser JM, Burant CF, Seino S, Mayo KE, et al. (1992) Glucose transporter expression in brain. cDNA sequence of mouse GLUT3, the brain facilitative glucose transporter isoform, and identification of sites of expression by in situ hybridization. J Biol Chem 267: 467-72.
13. Lanz TA, Carter DB, Merchant KM (2003) Dendritic spine loss in the hippocampus of young PDAPP and Tg2576 mice and its prevention by the ApoE2 genotype. Neurobiol Dis 13: 246-53.
14. Spires TL, Meyer-Luehmann M, Stern EA, McLean PJ, Skoch J, et al. (2005) Dendritic spine abnormalities in amyloid precursor protein transgenic mice demonstrated by gene transfer and intravital multiphoton microscopy. J Neurosci 25: 7278-87.
15. Tremblay ME, Riad M, Bouvier D, Murai KK, Pasquale EB, et al. (2007) Localization of EphA4 in axon terminals and dendritic spines of adult rat hippocampus. J Comp Neurol 501: 691-702.
16. Okabe T, Nakamura T, Nishimura YN, Kohu K, Ohwada S, et al. (2003) RICS, a novel GTPase-activating protein for Cdc42 and Rac1, is involved in the beta-catenin-N-cadherin and N-methyl-D-aspartate receptor signaling. J Biol Chem 278: 9920-7.
17. Bagni C, Greenough WT (2005) From mRNP trafficking to spine dysmorphogenesis: the roots of fragile X syndrome. Nat Rev Neurosci 6: 376-87.
18. Jourdain P, Fukunaga K, Muller D (2003) Calcium/calmodulin-dependent protein kinase II contributes to activity-dependent filopodia growth and spine formation. J Neurosci 23: 10645-9.
19. Sin WC, Haas K, Ruthazer ES, Cline HT (2002) Dendrite growth increased by visual activity requires NMDA receptor and Rho GTPases. Nature 419: 475-80.
20. Tashiro A, Yuste R (2004) Regulation of dendritic spine motility and stability by Rac1 and Rho kinase: evidence for two forms of spine motility. Mol Cell Neurosci 26: 429-40.
21. Holcomb L, Gordon MN, McGowan E, Yu X, Benkovic S, et al. (1998) Accelerated Alzheimer-type phenotype in transgenic mice carrying both mutant amyloid precursor protein and presenilin 1 transgenes. Nat Med 4: 97-100.
22. Hsia AY, Masliah E, McConlogue L, Yu GQ, Tatsuno G, et al. (1999) Plaque-independent disruption of neural circuits in Alzheimer's disease mouse models. Proc Natl Acad Sci U S A 96: 3228-33.
23. Marcotte ER, Srivastava LK, Quirion R (2001) DNA microarrays in neuropsychopharmacology. Trends Pharmacol Sci 22: 426-36.
24. Wu ZL, Ciallella JR, Flood DG, O'Kane TM, Bozyczko-Coyne D, et al. (2006) Comparative analysis of cortical gene expression in mouse models of Alzheimer's disease. Neurobiol Aging 27: 377-86.
25. Malinow R, Malenka RC (2005) AMPA receptor trafficking and synaptic plasticity. Annu Rev Neurosci 25: 103-26.
26. Shepherd JD, Huganir RL (2007) The cell biology of synaptic plasticity: AMPA receptor trafficking. Annu Rev Cell Dev Biol 23: 613-43.
27. Chang EH, Savage MJ, Flood DG, Thomas JM, Levy RB, et al. (2006) AMPA receptor downscaling at the onset of Alzheimer's disease pathology in double knockin mice. Proc Natl Acad Sci U S A 103: 3410-5.
28. Barria A, Muller D, Derkach V, Griffith LC, Soderling TR (1997) Regulatory phosphorylation of AMPA-type glutamate receptors by CaM-KII during long-term potentiation. Science 276: 2042-5.
29. McGlade-McCulloh E, Yamamoto H, Tan SE, Brickey DA, Soderling TR (1993) Phosphorylation and regulation of glutamate receptors by calcium/calmodulin-dependent protein kinase II. Nature 362: 640-2.
30. Murray KD, Isackson PJ, Jones EG (2003) N-methyl-D-aspartate receptor dependent transcriptional regulation of two calcium/calmodulin-dependent protein kinase type II isoforms in rodent cerebral cortex. Neuroscience 122: 407-20.
31. Amada N, Aihara K, Ravid R, Horie M (2005) Reduction of NR1 and phosphorylated Ca2+/calmodulin-dependent protein kinase II levels in Alzheimer's disease. Neuroreport 16: 1809-13.
32. Silva AJ, Paylor R, Wehner JM, Tonegawa S (1992) Impaired spatial learning in alpha-calcium-calmodulin kinase II mutant mice. Science 257: 206-11.
33. Silva AJ, Stevens CF, Tonegawa S, Wang Y (1992) Deficient hippocampal long-term potentiation in alpha-calcium-calmodulin kinase II mutant mice. Science 257: 201-6.
34. Reddy PH, McWeeney S, Park BS, Manczak M, Gutala RV, et al. (2004) Gene expression profiles of transcripts in amyloid precursor protein transgenic mice: up-regulation of mitochondrial metabolism and apoptotic genes is an early cellular change in Alzheimer's disease. Hum Mol Genet 13: 1225-40.
35. Manczak M, Anekonda TS, Henson E, Park BS, Quinn J, et al. (2006) Mitochondria are a direct site of A beta accumulation in Alzheimer's disease neurons: implications for free radical generation and oxidative damage in disease progression. Hum Mol Genet 15: 1437-49.